A Gray-Box Non-Parametric Aircraft System Identification Method Using the ANFIS Network for Prediction of High Angle of Attack Maneuvers

S. A. Bagherzadeh *, H. Mohammadkarimi[2]

[1] Department of Mechanical Engineering, Najafabad Branch, Islamic Azad University, Najafabad, Iran
[2] Department of Aerospace Engineering, Amirkabir University of Technology, Tehran, Iran

ABSTRACT: This paper aims to identify a gray-box non-parametric model for the airplane nonlinear aerodynamics throughout high angle of attack maneuvers using the Adaptive Neuro-Fuzzy Inference System (ANFIS). The gray-box modeling is employed in this paper in which the force and moments are predicted rather than the flight parameters. Flight test data of a large-scale unpowered model of a fighter airplane is modeled by ANFIS, and the results are compared with the traditional multi-layer feed forward Artificial Neural Network (ANN). The employed gray-box identification method considers both the nonlinearity and the longitudinal-lateral/directional coupling effects. The control commands and the flight conditions are the inputs to the system identification block while the force and moment coefficients are the targets. The optimal values for the ANFIS parameters are adjusted by the hybrid learning algorithm in order to minimize the Mean Squared Error (MSE) between the best estimated, target force, and moment coefficients while the ANN is trained by several learning algorithms. The precision of the model is checked during the training and test phases for a single flight condition. Afterwards, the generalization of the model is checked for flight conditions dissimilar from the training one. The results indicate that the ANN has moderate precision in the test phase while the ANFIS has excellent precision. Furthermore, based on the results, the ANN predictions cannot follow the flight data in flight conditions dissimilar from the training ones while the ANFIS seems quite robust in those conditions.

1- Introduction

So far, several mathematical methods have been employed to model nonlinear unsteady aerodynamics based on the flight tests performed at high angles of attack. Generally, the time-domain methods can be categorized into the parameter estimation and the system identification approaches. The first approach to the aircraft modeling is to estimate free parameters of a fixed aerodynamic model. The stability and control derivatives are the most commonly used aerodynamic model in the literature. Despite the straightforward mathematical base, the stability and control derivatives are not suitable for modeling high angle of attack flights. This is due to the fact that the first-order Taylor approximation is linear, and can capture neither nonlinearities nor couplings. In order to overcome this drawback, [1] divided the angle of attack range into some partitions, and obtained the stability and control derivatives for every local partition. Nevertheless, the partition method requires a large number of parameters, and may lack the prediction capability in many cases [2]. Additionally, the addition of higher order terms of the Taylor series to the aerodynamic model was studied by (i.e., the nonlinear and coupled terms) [3]. Since the number of the regressors increases exponentially with the polynomial order, the high or-

der models are physically insignificant [4]. Due to the aforementioned drawbacks, the conventional stability and control derivatives are much more common in the literature than the partition and high order models. There are many recent researches conducted about the estimation of the conventional stability and control derivatives. In these studies, a variety of sophisticated mathematical tools are employed, such as the Artificial Neural Networks (ANNs) ([5]-[9]), Support vector machine [10], Kalman filter ([11], [12], optimal control [13], and fuzzy methods ([14], [15]). It should be noted that the structure of the conventional stability and control derivatives is not able to capture the nonlinear and coupled behaviors. Therefore, the parametric models are not suitable to model high angle of attack maneuvers, no matter what the parameter estimation mathematical method is employed.

The second approach to the aircraft modeling is the system identification in which the structure selected as the aerodynamic model is not pre-determined. Instead, the model structure is flexible enough to capture complicated phenomena. This purpose can be achieved using so-called non-parametric models, in which the selected structure has either several free parameters or a data-driven base. The system identification approach is not dependent on the model structure. Thus, it is a suitable choice to predict high angle

*Corresponding author's email: bagherzadeh@pmc.iaun.ac.ir

of attack maneuvers. So far, several mathematical tools have been employed as the non-parametric models for the aircraft system identification, such as the Gaussian processes [16], the wavelet [17], the ANN [18], the Support Vector Machine (SVM) ([19]) and the fuzzy models ([20], [21], [22] , [23]). In many cases, the non-parametric models get into difficulty with the generalization. In other words, some non-parametric models are satisfactorily trained. Nevertheless, their performances degrade in dealing with non-trained flight test data obtained at flight conditions dissimilar from the training ones. To overcome this drawback, the gray-box modeling is used, in which the force and moments are predicted rather than the flight parameters. Afterwards, the equations of motion are utilized for the prediction of the flight parameters. The gray-box models have acceptable properties from the generalization as well as the precision viewpoints [4]. In this paper, a gray-box non-parametric aircraft system identification method is proposed for high angle of attack maneuvers using the Adaptive Network-based Fuzzy Inference System (ANFIS) network.

The ANFIS network is a method for approximating complicated nonlinear function. This method contains a fuzzy inference system based on fuzzy rules in which the Membership Functions (MFs) are selected by ANN. ANFIS network combines both fuzzy logic and ANN; therefore, it may benefit from their advantages. The most outstanding feature of the ANFIS network is that it is a universal estimator [24]. In other words, the ANFIS network can estimate any arbitrary piecewise continuous function with any desired precision. This feature makes the ANFIS network one of the best methods for the aircraft system identification, especially for high angle of attack flights. In recent years, the ANFIS network is employed for the aerodynamic parameter estimation [25]-[28]. However, up to the author's best knowledge, it has not been employed for the aircraft system identification until now. In this paper, the ANFIS network is proposed as a gray-box non-parametric aircraft system identification method for the prediction of high angle of attack flights for the first time.

The remainder of the paper is organized as follow: First, a brief review of the ANFIS network is presented. Afterwards, the system identification and simulation processes are introduced. Later, the proposed method is applied to the flight test data of a Remotely Piloted Vehicle (RPV), and the results are compared with the traditional ANN. Finally, conclusions are presented.

2- The ANFIS Network

The ANFIS network consists of artificial neurons organized in a 5-layer structure. Suppose the ordered pair (x,y), in which $\mathbf{x} = [x_1 \cdots x_n] \in U \subset \Re^n$ is the input vector and $y \in V \subset \Re$ is the output vector. Additonally, suppose that there are p Sugeno-type fuzzy rules, as follows:

$$Ru^{(i)}: \text{ if } x_1 \text{ is } A_1^i \text{ and } \cdots \text{ if } x_n \text{ is } A_n^i \text{ then } f_i = \sum_{k=1}^n q_{ik}x_k + r_i \quad (1)$$

where $i = 1, \cdots, p$.

Until now, several structures are proposed for the ANFIS network. One of the most common structures for is described here:

• **Layer 1:** This layer performs the fuzzification process using the MFs $\mu_{i,j}(x_j)$, where $j = 1, \cdots, n$ and $i = 1, \cdots, p$. Thus, there are $n.p$ MFs with the input x_j and the output $\mu_{i,j}(x_j)$. Any parameterized MF can be utilized in this layer. For instance, the bell-shaped MFs can be used in this layer, as follows:

$$\mu_{i,j}(x_j) = \frac{1}{1 + \left|\frac{x_j - c_{i,j}}{a_{i,j}}\right|^{2b_{i,j}}} \quad (2)$$

in which the premise parameters a, b and c define the form of the bell-shaped MFs.

• **Layer 2:** This layer determines the firing power of the fuzzy rules by a T-norm operator. In this paper, a product inference engine is employed that multiplies all of its inputs, as follows:

$$w_i = \prod_{j=1}^n \mu_{ij} \quad , \quad i = 1, \cdots, p \quad (3)$$

Layer 2 does not contain free parameters.

• **Layer 3:** This layer normalizes the firing power of the fuzzy rules, as follows:

$$\overline{w}_i = \frac{w_i}{\sum_{k=1}^p w_k} \quad , \quad i = 1, \cdots, p \quad (4)$$

Similar to the previous layer, Layer 3 does not contain free parameters. The normalized firing strengths are usually represented by the operator N.

• **Layer 4:** This layer calculates the crisp outputs using the weighted average by the function f_i, as follows:

$$z_i = \overline{w}_i f_i \quad , \quad i = 1, \cdots, p \quad (5)$$

In which f_i may be defined as follows:

$$f_i = \sum_{k=1}^n q_{ik}x_k + r_i \quad (6)$$

where the consequent parameters q and r are free parameters.

• **Layer 5:** This layer finds the summation of the difuzzified values, as follows:

$$y = \sum_{i=1}^p z_i \quad (7)$$

Layer 5 does not contain free parameters.

The flowchart of the ANFIS network is illustrated in Fig. 1.

The premise parameters a, b and c as well as the consequent parameters q and r should be selected in a way that the error between the predicted and measured values are minimized. To that end, several numerical techniques can be employed. In this paper, the *hybrid learning* is used in which both the least squares and the steepest descent techniques are simultaneously utilized.
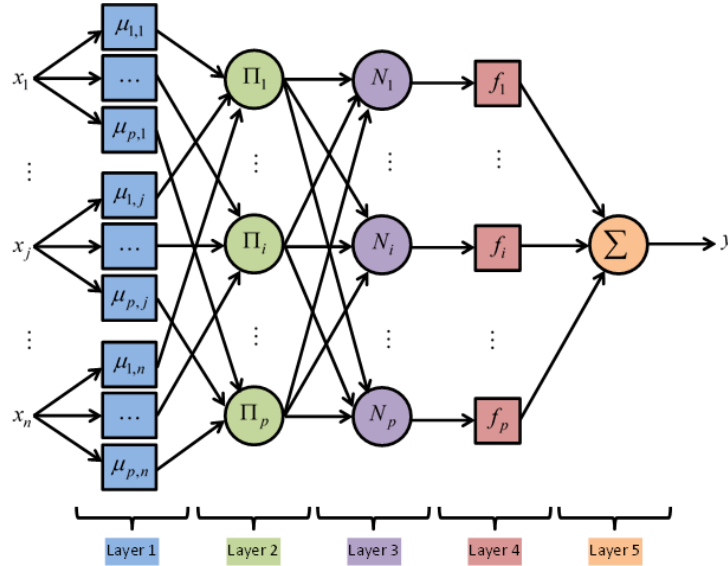

Fig. 1. The flowchart of the ANFIS network

3- The System Identification
3- 1- The Aircraft

In this paper, flight test data presented by [29] is examined. The aircraft studied in this reference was a RPV that is a 3/8 scale of a twin-engine double fin fighter. The RPV was unpowered, and was launched from another airplane. During the flight, the RPV was able to perform extremely high angle of attack maneuvers. The studied RPV had the following characteristics:

Table 1. The characteristics of the RPV studied by [29]

Parameter	Value	Unit
m	842	kg
S	7.94	m^2
$\bar{c}$	1.82	m
b	4.89	m
I_{xx}	256	$kg.m^2$
I_{yy}	1650	$kg.m^2$
I_{zz}	1880	$kg.m^2$
I_{xz}	-10	$kg.m^2$
$\bar{X}_{CG}$	26	$\%MAC$

3- 2- Equations of Motion

During the aircraft system identification, the inputs and targets for the model should be determined. In the error equation method, the aerodynamic forces and moment coefficients are considered as the dependent variables (i.e., targets of the model), while the measured flight data are considered as the independent variables (i.e., inputs to the model). The error equation method is a gray-box system identification method in which both the Equations of Motion (EOM) governing the aircraft dynamics and the input-output measured data are used in the modeling process. Since the aerodynamic force and moment coefficients cannot directly be measured, one may need the inverse EOM that calculates the force and moment coefficients based on the flight parameters, as follows:

$$C_X = \frac{m}{\bar{q}S}\left[\begin{array}{l}(\dot{u} + g\sin\theta - rv + qw)\cos\alpha \\ + (\dot{w} - g\cos\theta\cos\phi - qu + pv)\sin\alpha\end{array}\right]$$

$$C_Y = \frac{m}{\bar{q}S}[\dot{v} - g\cos\theta\sin\phi + ru - pw]$$

$$C_Z = \frac{m}{\bar{q}S}\left[\begin{array}{l}-(\dot{u} + g\sin\theta - rv + qw)\sin\alpha \\ + (\dot{w} - g\cos\theta\cos\phi - qu + pv)\cos\alpha\end{array}\right]$$

$$C_l = \frac{1}{\bar{q}Sb}\left[I_{xx}\dot{p} - I_{xz}\dot{r} - I_{xz}pq + (I_{zz} - I_{yy})qr\right]$$

$$C_m = \frac{1}{\bar{q}S\bar{c}}\left[I_{yy}\dot{q} + (I_{xx} - I_{zz})pr + I_{xz}(p^2 - r^2)\right]$$

$$C_n = \frac{1}{\bar{q}Sb}\left[I_{zz}\dot{r} - I_{xz}\dot{p} + I_{xz}qr + (I_{yy} - I_{xx})pq\right]$$

(8)

It should be mentioned that the angle of attack, sideslip angle, Euler angles, angular rates and translational accelerations are directly measured by the flight data acquisition system [29], while the time derivatives of the angular rates should be calculated by numerical derivative methods.

In addition, the direct EOMs are required to map the estimated force and moment coefficients into the estimated flight parameters. The direct EOM is a set of first-order coupled nonlinear differential equations governing the translational and rotational dynamics of an aircraft. These equations calculate the rate of change of the translational and angular velocity components from the forces and moment coefficients. The direct EOM is represented as follows:(9)

$$\hat{u} = \frac{\bar{q}S}{m}\left(\hat{C}_X \cos\alpha - \hat{C}_Z \sin\alpha\right) - g\sin\theta + rv - qw$$

$$\hat{v} = \frac{\bar{q}S}{m}\hat{C}_Y + g\cos\theta\sin\phi - ru + pw$$

$$\hat{w} = \frac{\bar{q}S}{m}\hat{C}_Z\left(\hat{C}_X \sin\alpha + \hat{C}_Z \cos\alpha\right) + g\cos\theta\cos\phi + qu - pv$$

$$\hat{p} = \frac{1}{I_{xx}I_{zz} - I_{xz}^2}\begin{bmatrix} \bar{q}Sb\left(I_{zz}\hat{C}_l + I_{xz}\hat{C}_n\right) \\ + pq\left(I_{xx}I_{xz} - I_{yy}I_{xz} + I_{zz}I_{xz}\right) \\ + qr\left(I_{yy}I_{zz} - I_{zz}^2 - I_{xz}^2\right) \end{bmatrix}$$

$$\hat{q} = \frac{1}{I_{yy}}\left[\bar{q}Sc\hat{C}_m + I_{xz}\left(r^2 - p^2\right) + \left(I_{zz} - I_{xx}\right)pr\right]$$

$$\hat{r} = \frac{1}{I_{xx}I_{zz} - I_{xz}^2}\begin{bmatrix} \bar{q}Sb\left(I_{xz}\hat{C}_l + I_{xx}\hat{C}_n\right) \\ + pq\left(I_{xx}^2 + I_{xz}^2 - I_{xx}I_{yy}\right) \\ + qr\left(I_{yy}I_{xz} - I_{zz}I_{xz} - I_{xx}I_{xz}\right) \end{bmatrix}$$

$$(9)$$

Using the numerical integration methods, one can find the estimated translational and angular velocity components (i.e., $\hat{u}$, $\hat{v}$, $\hat{w}$, $\hat{p}$, $\hat{q}$ and $\hat{r}$) throughout the desired time interval. Additionally, the rate of changes of the Euler angles can be obtained by the following equations:

$$\hat{\dot{\phi}} = \hat{p} + \hat{q}\sin\hat{\phi}\tan\hat{\theta} + \hat{r}\cos\hat{\phi}\tan\hat{\theta}$$

$$\hat{\dot{\theta}} = \hat{q}\cos\hat{\phi} - \hat{r}\sin\hat{\phi}$$

$$\hat{\dot{\psi}} = \frac{\hat{q}\sin\hat{\phi} + \hat{r}\cos\hat{\phi}}{\cos\hat{\theta}}$$

$$(10)$$

Furthermore, the rate of change of the altitude can be found as follows:

$$\hat{\dot{h}} = -\hat{u}\sin\hat{\theta} + \hat{v}\sin\hat{\phi}\cos\hat{\theta} + \hat{w}\cos\hat{\phi}\cos\hat{\theta} \qquad (11)$$

The numerical integration methods are needed to obtain the Euler angle as well as the altitude throughout the desired time interval.

3- 3- The Gray-Box Identification Process

The proposed gray-box identification process is illustrated in Fig. 2. As can be seen, the flight parameters X(t), the control commands U(t), and the flight conditions F(t) are the inputs to the system identification block. The inputs are defined as follows:

$$X(t) = \begin{bmatrix} \alpha(t) & \beta(t) & \phi(t) & \theta(t) & a_x(t) & a_y(t) & a_z(t) & p(t) & q(t) & r(t) \end{bmatrix}^T$$

$$U(t) = \begin{bmatrix} \delta_A(t) & \delta_E(t) & \delta_R(t) \end{bmatrix}^T \qquad (12)$$

$$F(t) = \begin{bmatrix} V(t) & h(t) \end{bmatrix}^T$$

Moreover, the force and moment coefficients $C(t)$ are the targets for the identification block. The target vector is defined as follows:

$$\mathbf{C}(t) = \begin{bmatrix} C_X(t) & C_Y(t) & C_Z(t) & C_l(t) & C_m(t) & C_n(t) \end{bmatrix}^T \quad (13)$$

In the proposed gray-box identification process, one may need the inverse EOM (i.e., Eq. 8) to obtain the target parameters. The Euler angles, the translational acceleration components, the angle of attack, and the sideslip angle are measured during the flight tests while the angular acceleration components are calculated by applying the smoothed numerical differentiation to the angular rates. Additionally, the weight and the moments of inertia are obtained by ground tests, as indicated in Table 1.

Once the inputs and targets are provided, the proposed gray-box system identification block attempts to find the optimal values for the ANFIS structure. To that end, it is necessary to minimize the Mean Squared Error (MSE) between the best estimated force and moment coefficients $\hat{C}(t)$ and the target force and moment coefficients $C(t)$. In order to find the optimal ANFIS parameters, they should be adjusted by a training rule. In this paper, the hybrid learning is employed in which both the least squares and the steepest descent techniques are simultaneously utilized.

The best estimated force and moment coefficients $\hat{C}(t)$ are the output of the gray-box system identification block. Afterwards, it is straightforward to estimate the derivatives of the flight parameters $\hat{X}(t)$ using the direct EOM of Eqs. 9 to 11. Finally, the numerical integration is utilized to find the estimated flight parameters $\hat{X}(t)$.

When the identification process is completed, the resultant model can be utilized for simulating both the trained and non-trained flight tests. For the flight simulation, the ANFIS structure containing the optimal parameters is used. The simulation process is illustrated in Fig. 3. The control commands $U(t)$, and the estimated flight parameters $\hat{X}(t)$ at the previous time step are the inputs to the model, while the estimated force and moment coefficients $\hat{C}(t)$ are the outputs. Afterwards, derivatives of the flight parameters $\hat{X}(t)$ are estimated using direct EOM (i.e., Eqs. 9 to 11). Finally, the numerical
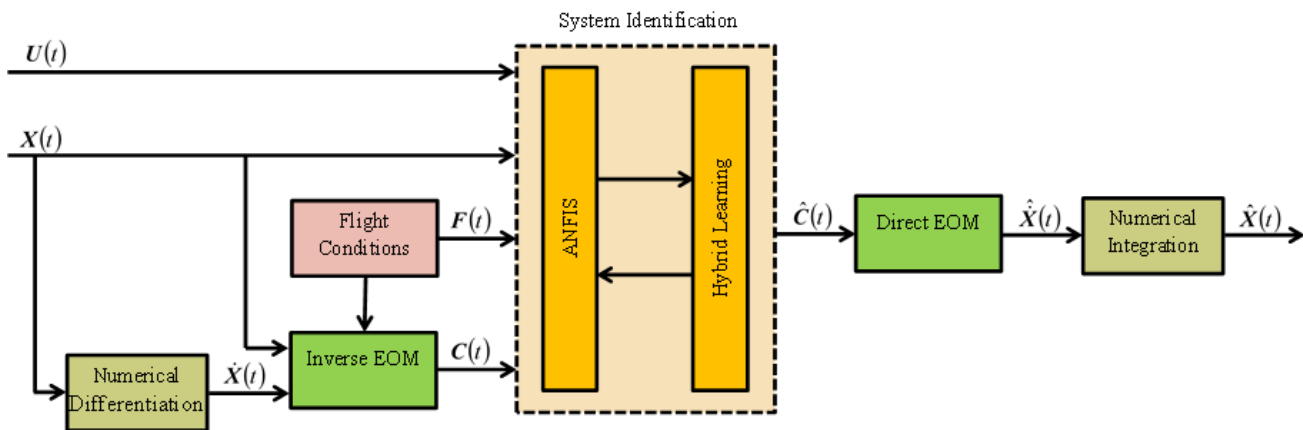
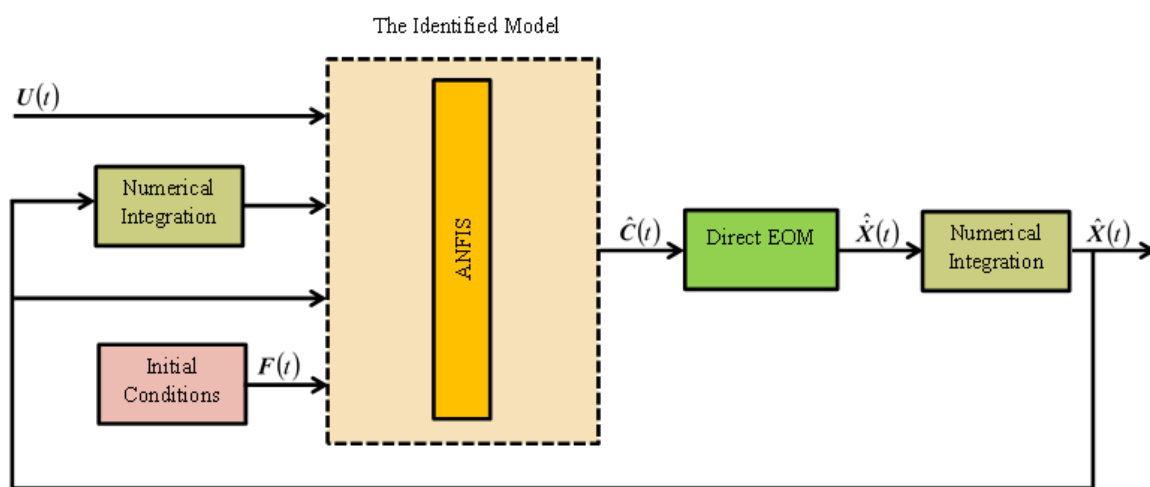**Fig. 2. The gray-box identification process**

Fig. 3. The simulation process

integration is required to find the estimated flight parameters $\hat{X}(t)$. In addition, numerical integration is employed to determine the flight conditions for the next time step. It can be observed that there is a loop for the simulation in which the flight condition needed at every time step is calculated at the previous one; therefore, an initial condition is needed to start the loop.

4- Results and Discussion

In this section, the ANFIS identification process proposed in the previous section is employed to identify the nonlinear aerodynamics of the RPV studied by [29]. The identification and simulation processes using the ANFIS network is performed according to Figs. 2 and 3, respectively. The employed ANFIS structure contains first order Sugeno-type systems of Eq. (1) with the weighted average defuzzification. The rule sharing is not applied to the ANFIS structure. Two bell-shaped MFs are implemented in Layer 1 for every input. The initial step size is selected 0.01 while it is changed by 10% at every epoch during the training process.

An ANN is also applied to the same aircraft system identification problem for comparison. The identification and simulation processes using the ANN are very similar to Figs. 2 and 3, except that the ANFIS network within the models are replaced by the ANN. The employed ANN has a two-layer feed-forward architecture adjusted for the input-output curve fitting. The hidden layer of the ANN contains 16 neurons with the sigmoid activation functions, while the output layer has a linear transfer function. The weights and biases of the network are tuned by the Levenberg-Marquardt backpropagation training algorithm. The dataset is randomly divided in a way that 70% of the input-target ordered pairs are used for the training phase while 15% is used for the validation phase, and the remainder for the test phase. Additionally, the initial conditions of the ANN are randomly selected.

The performance of the ANFIS and ANN is measured using the Root-Mean-Square Error (RMSE) and Fit Percentage (FP) criteria, as follows:

$$RMSE = \left(\frac{1}{n} \sum_{i=1}^{n} \left(y_i - \hat{y}_i \right)^2 \right)^{1/2}$$

$$FP = 100\% \left(1 - \frac{\left(\sum_{i=1}^{n} \left(y_i - \hat{y}_i \right)^2 \right)^{1/2}}{\left(\sum_{i=1}^{n} \left(y_i - \bar{y} \right)^2 \right)^{1/2}} \right) \qquad (14)$$

In which $\bar{y} = \dfrac{\sum_{i=1}^{n} y_i}{n}$, y is the measured target, and $\hat{y}$ is the corresponding model output.

4- 1- The Precision of the Model

The time-histories of the flight parameters in pull ups and turns to high angle of attack maneuvers acquired at the initial altitude of 10500 m is illustrated in Fig. 4 [29].

For training and test phases, the flight data is divided up into two segments: The first segment contains 60 seconds of the time-histories, while the second one contains the remaining 40 seconds. The time-histories include the flight parameters $X(t)$, the control commands $U(t)$, and the flight conditions $F(t)$ as introduced by Eq. (12). The training segments of the time-histories are the input to the identification process (i.e., Fig. 2). Additionally, the target force and moment coefficients $C(t)$ calculated by the inverse EOM are the targets for the system identification block. Within the training phase, the free parameters of the ANN and ANFIS models are selected so that the RMSEs between the best estimated force and moment coefficients $\hat{C}(t)$ and the target force and moment coefficients $C(t)$ are minimized. Therefore, the flight parameters are not directly comparable during the training phase. The flight parameters are the outputs of the direct EOM and numerical integrations based on the initial conditions. The learning rules are needed to adjust the free parameters of the models (i.e., the ANN and ANFIS) throughout the training phase. The test segments of time-histories are the input to the simulation process (i.e., Fig. 3), while there is no target for the models. For the test phase, the trained models are employed to predict the force and moment coefficients based on the control commands. The previous values of the flight parameters and the flight conditions are also needed for the simulation. These values are obtained by the numerical integrations based on the initial conditions.

The regression plots for the force and moment coefficients estimated by ANN are illustrated in Fig. 5. In these figures, the estimated force and moment coefficients are plotted against the corresponding target values for the training and test phases. It can be observed that the slopes and the biases of the ANN regression plots for the training phase are almost 1 and 0, respectively. Therefore, ANN has almost a perfect predic-

tion for the trained dataset. On the contrary, the slopes and the biases of the ANN regression plots diverge from their ideal values (i.e., 1 and 0, respectively) for the test dataset. In other words, the performance of ANN is degraded when it faces non-trained input values. Additionally, the distribution of the points within the regression plots indicate that the relationships between the model outputs and targets are weakened for the test datasets. Based on the results, one can conclude that ANN encounters the over-fitting, namely the condition in which the model has acceptable performance throughout the training while its outputs diverge from the targets in dealing with non-trained inputs. The over-fitting problem of ANN for the aircraft system identification was previously reported by [18]. Therefore, ANN is not a suitable non-parametric model for the aircraft modeling.

The regression plots for the force and moment coefficients estimated by ANFIS are illustrated in Fig. 6. It can be seen that the slopes and the biases of the ANFIS regression plots are very close to the ideal values for both the training and test phases (i.e., 1 and 0, respectively). Additionally, the distributions of the points around the regression lines indicate strong relationships between the model outputs and targets. Therefore, the ANFIS performance is acceptable in the training and test phases. It can be observed that ANFIS does not encounter with over-fitting problem.

The time-histories of the estimated force and moment coefficients for ANN and ANFIS models are illustrated in Figs. 7 and 8. In these figures, the target force and moment coefficients as well as the estimated force and moment coefficients within the training and test phases are depicted. As can be observed, the time-histories predicted by the ANN and ANFIS models are very similar to the target ones. Thus, the training phases are fairly successful for both ANN and ANFIS models. On the contrary, the test phase of ANN does not completely coincide with the targets while ANFIS is much more successful at predicting the time-histories. The RMSE and FP values for the time-histories predicted by ANN and ANFIS models are listed in Tables 2 and 3.

The regression plots for the flight parameters obtained by ANN and ANFIS are illustrated in Figs. 9 and 10, respectively. These regression plots represent the estimated flight parameters against the measured ones. Both the training and test phases are shown in the regression plots. As can be seen, the ANN performance is almost perfect during the training phase since the regression lines are similar to the identity line. However, the ANN capability for the prediction of the flight parameters declines within the test phase. For the test phase, it can be observed that the regression lines do not remain similar to the identity line. On the contrary, it can be seen that ANFIS can precisely predict the flight parameters in the training as well as the test phases. For ANFIS, the distribution of the points represents strong relationships between the model outputs and targets for both the training and test phases.
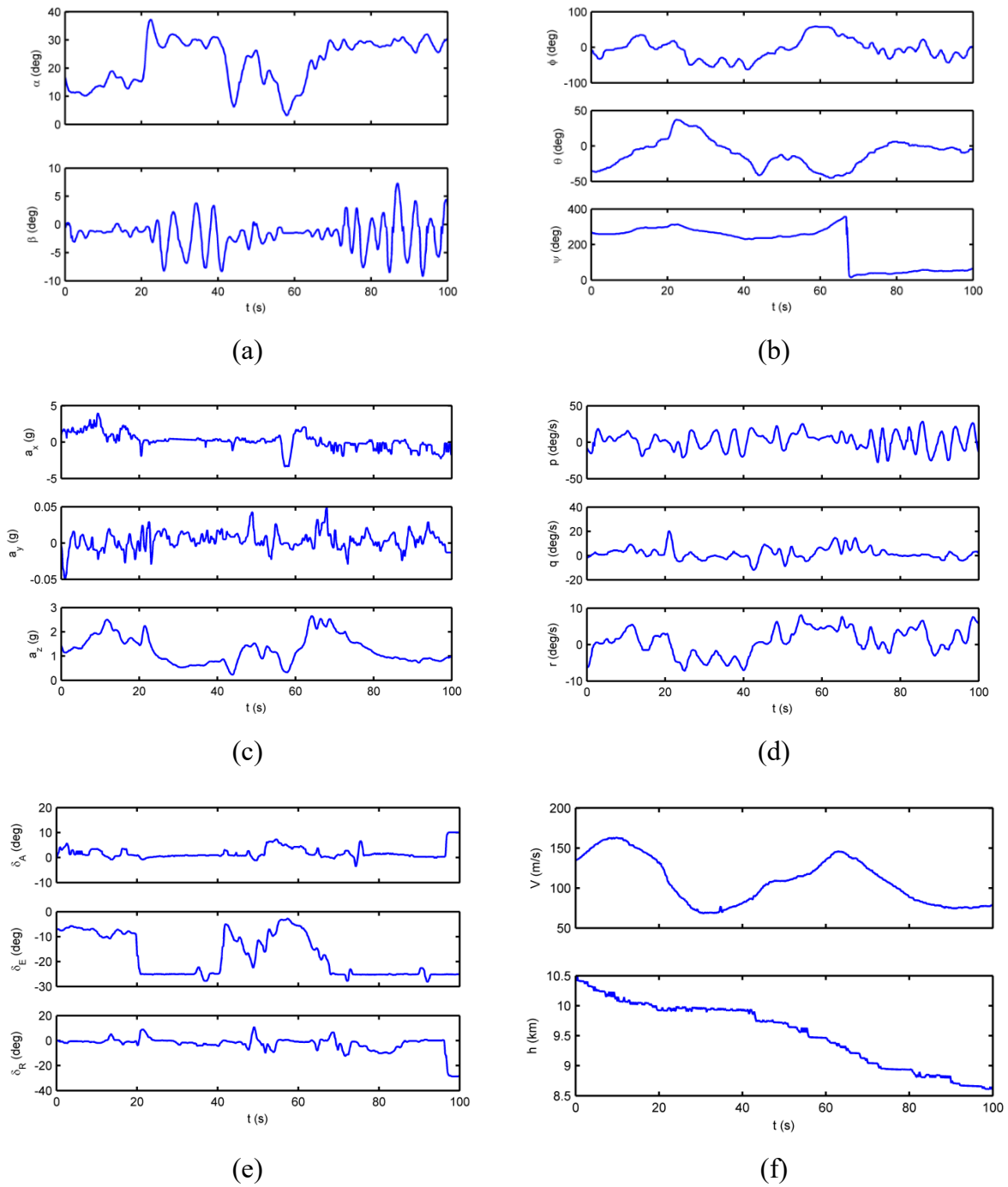
Fig. 4. The time-histories of the flight parameters in pull ups and turns to high angle of attack maneuvers: (a) flight angles, (b) Euler angles, (c) translational accelerations, (d) rotational velocities, (e) control commands, (f) flight conditions [29]
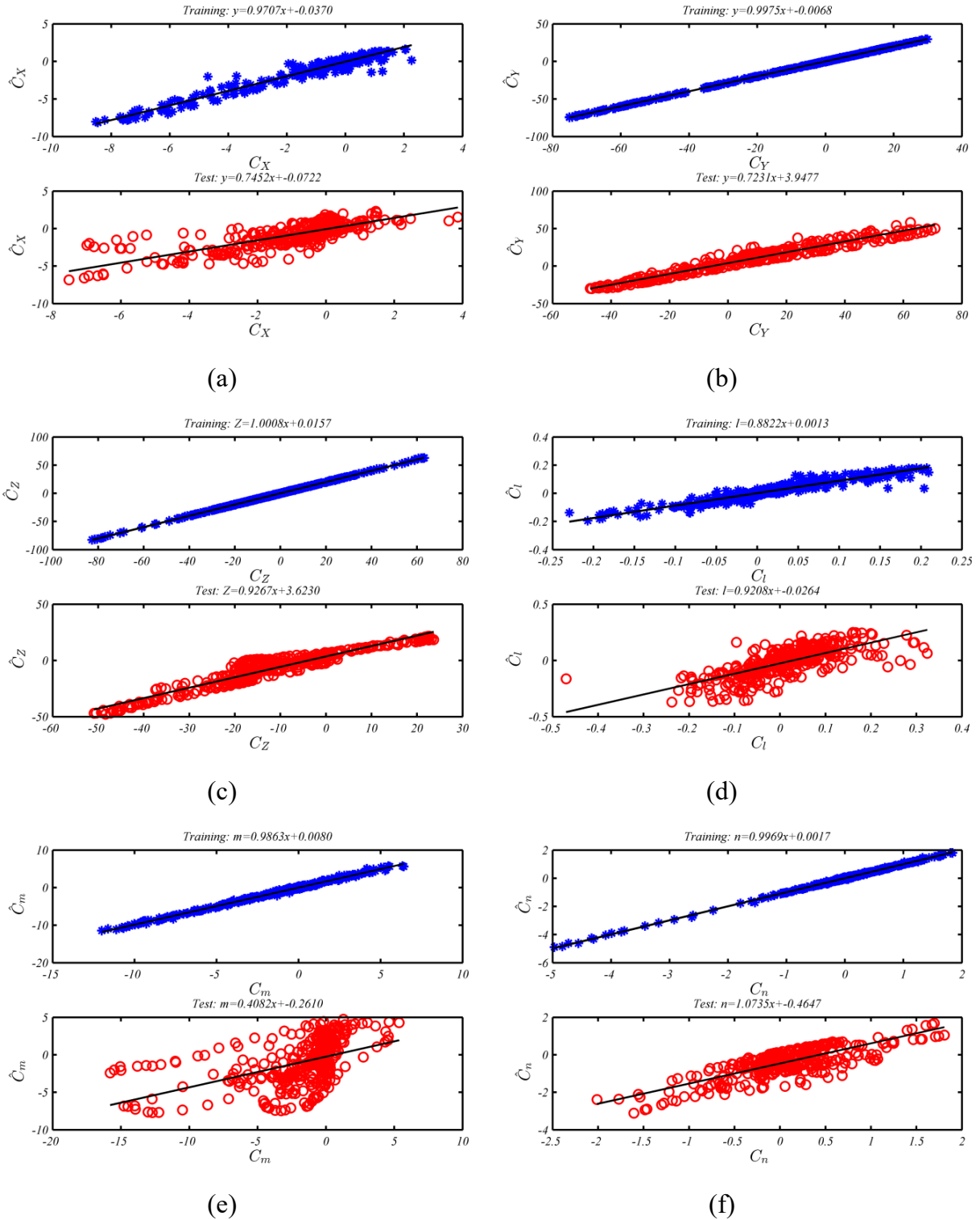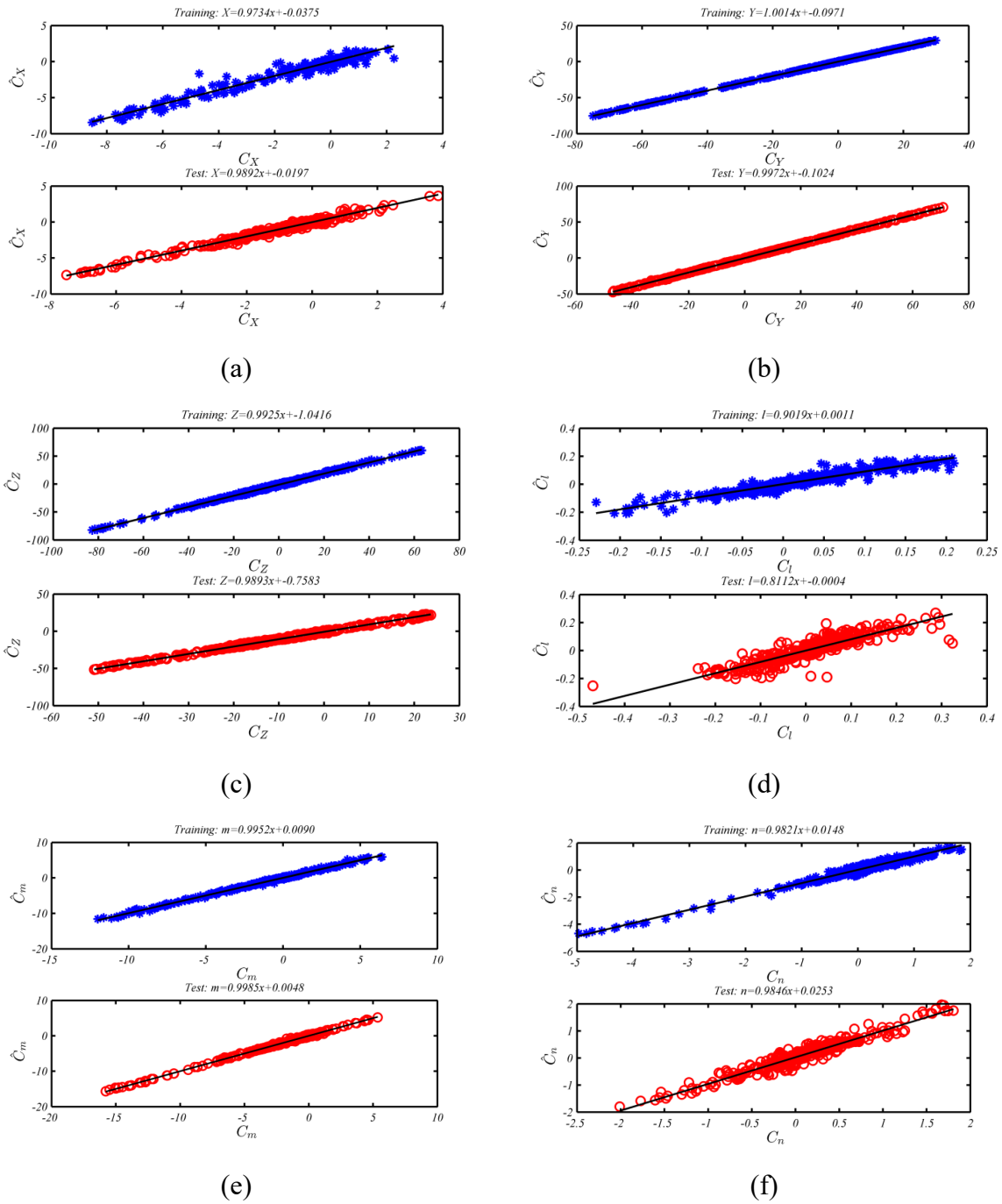
(a)

(b)

(c)

(d)

(e)

(f)

Fig. 5. The regression plots for the force and moment coefficients estimated by the ANN

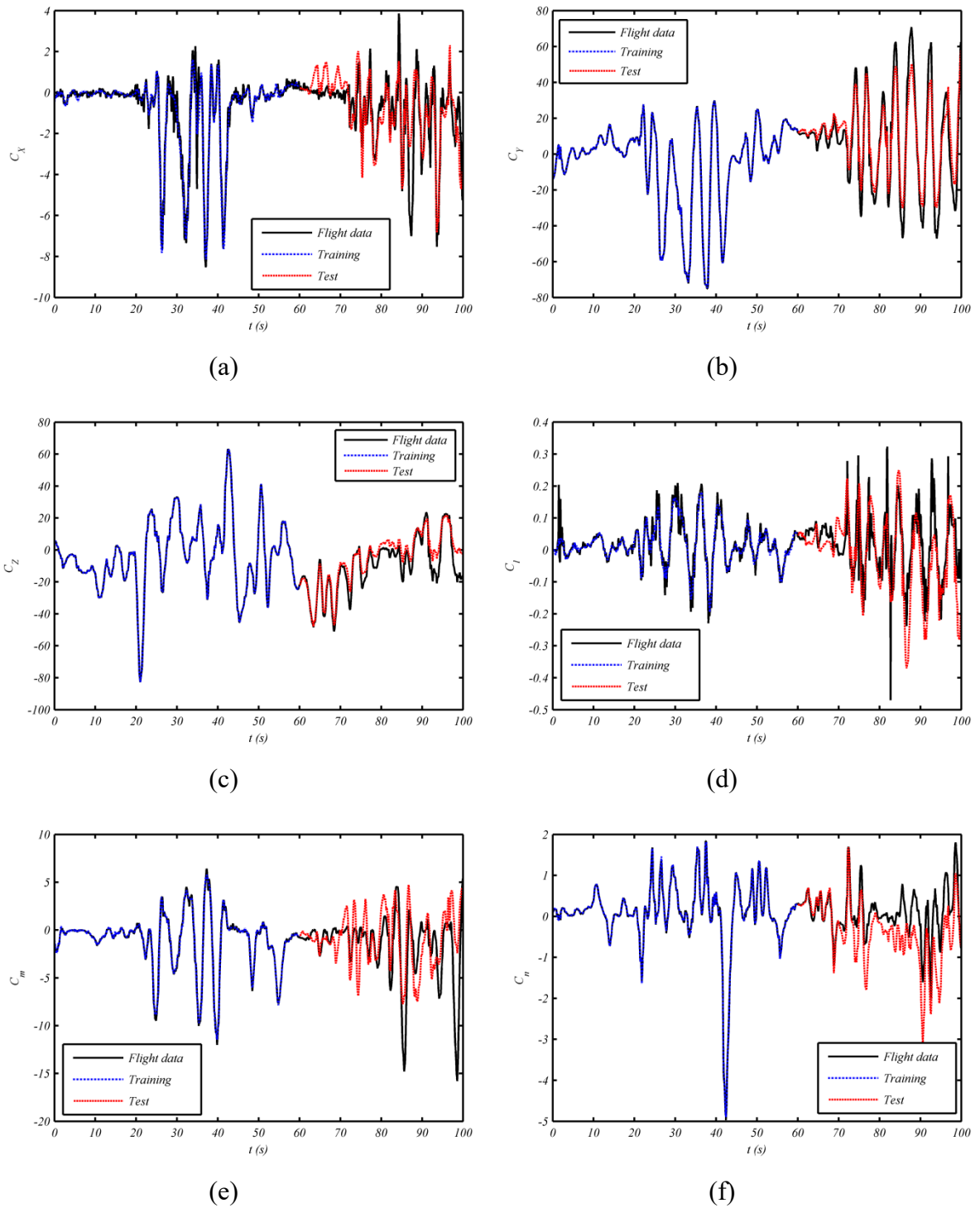Fig. 6. The regression plots for the force and moment coefficients estimated by the ANFIS

Fig. 7. The time-histories of the force and moment coefficients estimated by the ANN model
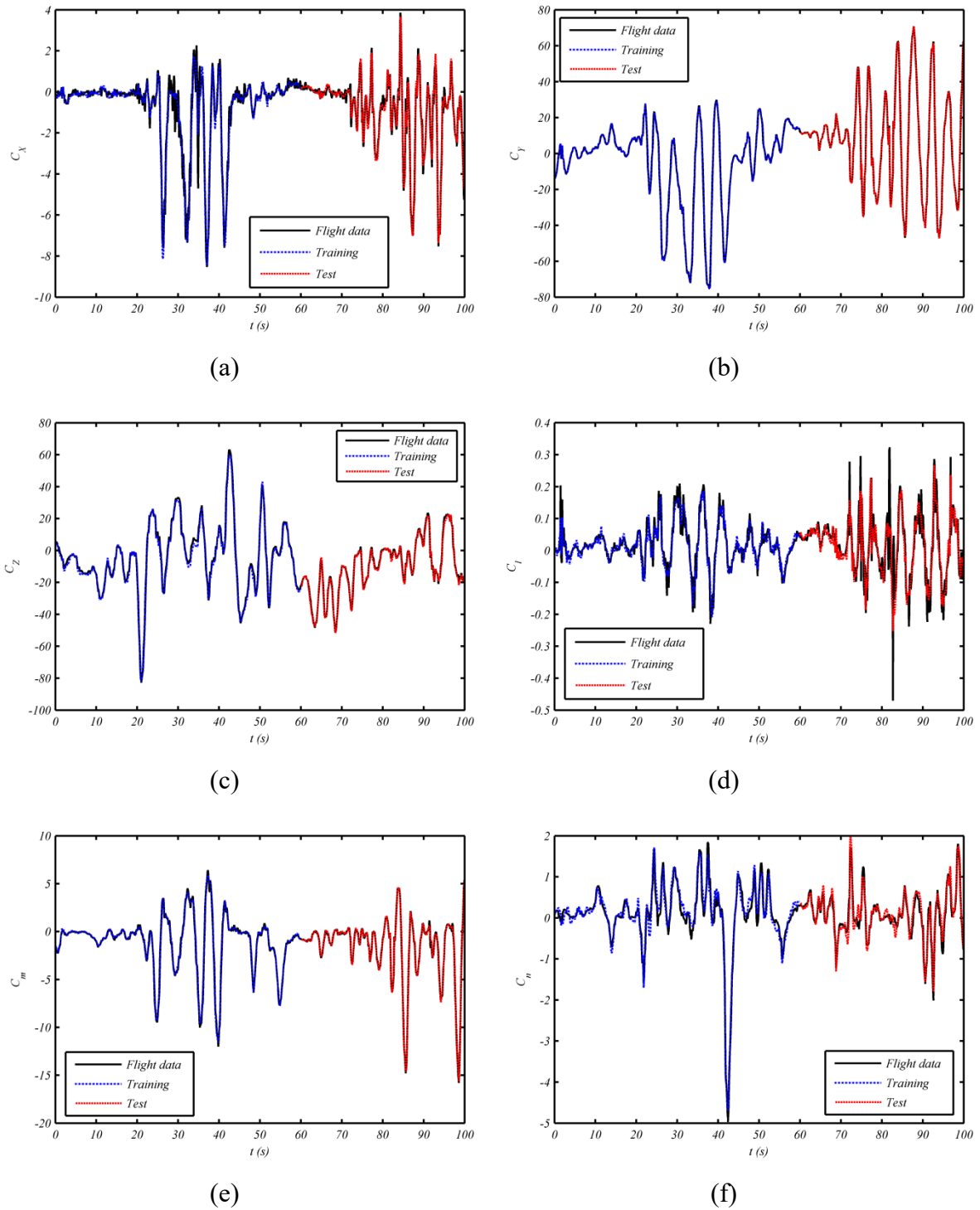
Fig. 8. The time-histories of the force and moment coefficients estimated by the ANFIS model

Table 2. The RMSE and FP for time-histories of the force and moment coefficients estimated by the ANN model

	Training		Test	
	RMSE	FP	RMSE	FP
C_X	0.3842	79.5288	1.0952	37.5574
C_Y	0.2398	98.9617	8.7096	67.1025
C_Z	0.2813	98.6939	6.5773	59.9652
C_l	0.0216	67.1468	0.0895	7.7543
C_m	0.2070	92.9950	3.2313	5.6729
C_n	0.0313	96.2152	0.6512	18.6755

Table 3. The RMSE and FP for time-histories of the force and moment coefficients estimated by the ANFIS model

	Training		Test	
	RMSE	FP	RMSE	FP
C_X	0.3548	81.0963	0.2282	86.9907
C_Y	0.2453	98.9380	0.4236	98.3999
C_Z	1.5386	92.8563	1.1100	93.2436
C_l	0.0212	87.6975	0.0440	84.6019
C_m	0.2025	93.1464	0.1622	95.2658
C_n	0.1464	82.2932	0.1423	84.0737

The time-histories of the flight parameters acquired by ANN and ANFIS are illustrated in Figs. 11 and 12, respectively. In these figures, the target flight parameters as well as the estimated ones are depicted throughout the training and test phases. The outstanding performance of ANFIS in comparison with ANN can be observed in these figures, especially for the test phase. The RMSE and FP values for the time-histories predicted by ANN and ANFIS models are represented in Tables 4 and 5, respectively.

4- 2- The Generalization of the Model

The aircraft model acquired by the identification process should be valid for flight conditions dissimilar from the training one. In other words, the model should have acceptable generalization not only for dissimilar input commands, but also for different flight conditions. In this subsection, ANN and ANFIS models (trained at the altitude of 10500 m) are used for the simulation of the flight parameters acquired at the initial altitude of 17000 m. Therefore, there is no training phase, and the models obtained at the previous sub-section are employed for the simulation. The time-histories of the flight parameters acquired by ANN and ANFIS models as well as the flight data are illustrated in Fig. 13. Additionally, the RMSE and FP values for the time-histories predicted by ANN and ANFIS for the flight test data acquired at the initial altitude of 17000 m are listed in Table 6.
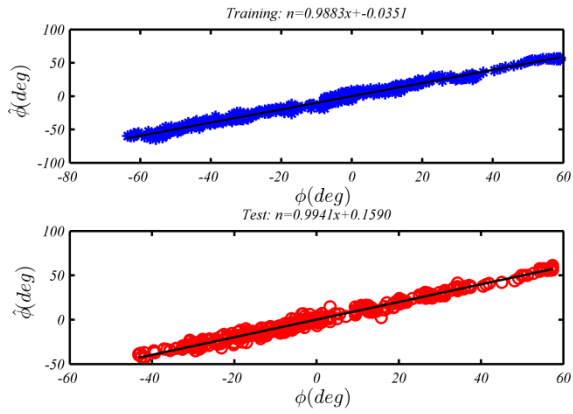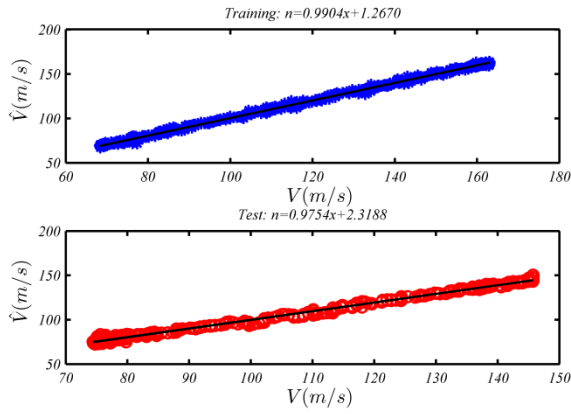
(a)

(b)

(c)

(d)

(e)
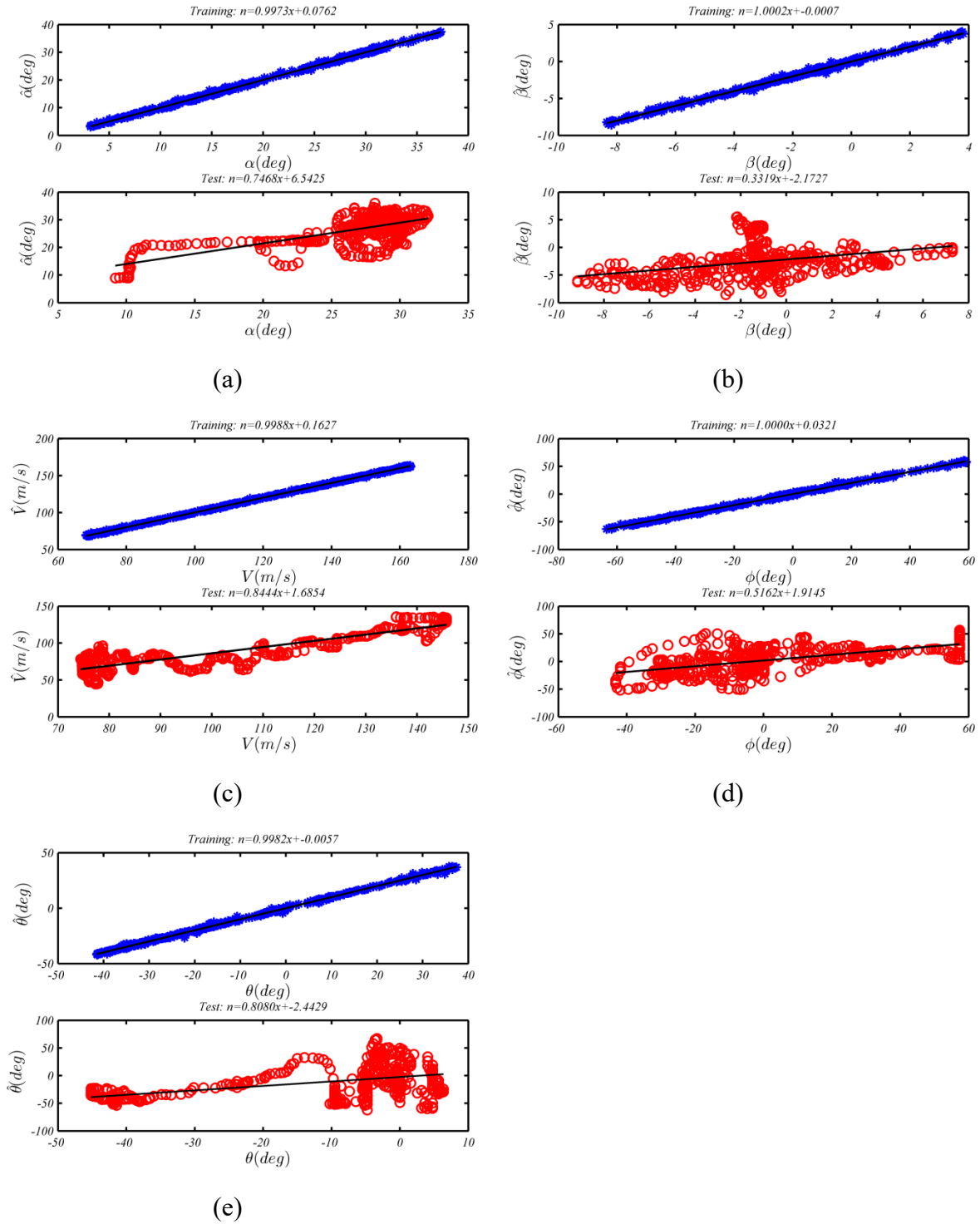
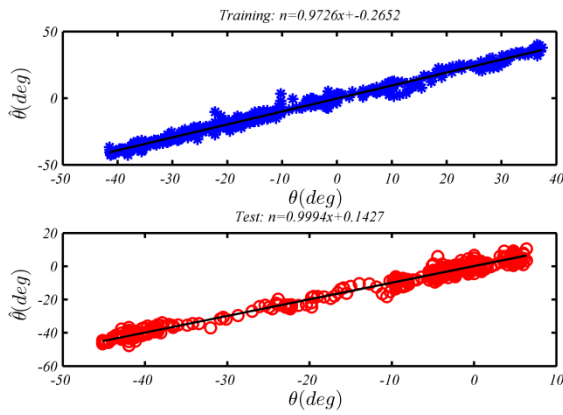**Figs. 9. The regression plots for the flight parameters obtained by the ANN**
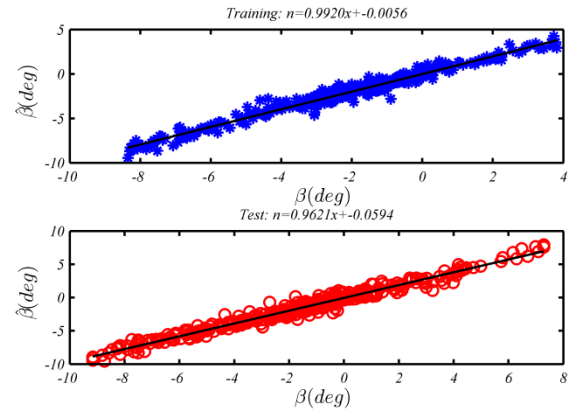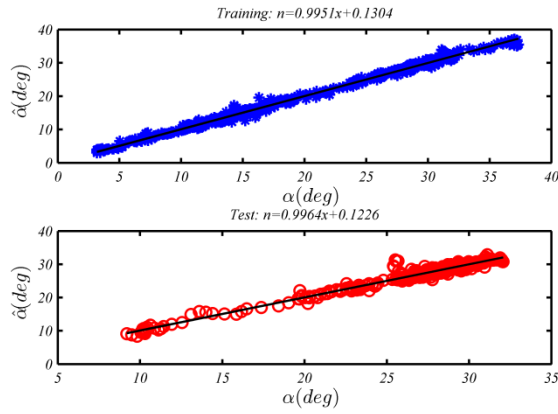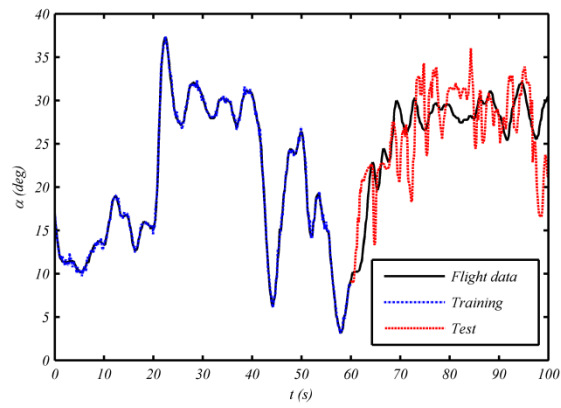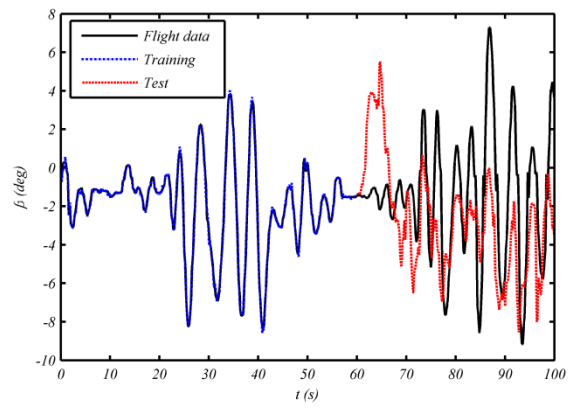
(a)

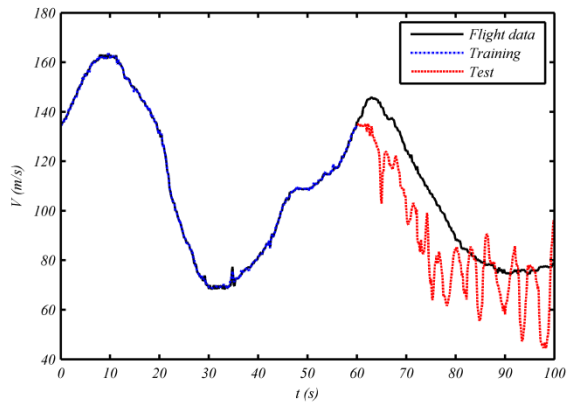(b)

(c)

(d)

(e)

Figs. 10. The regression plots for the flight parameters obtained by the ANFIS

(a)

(b)

(c)
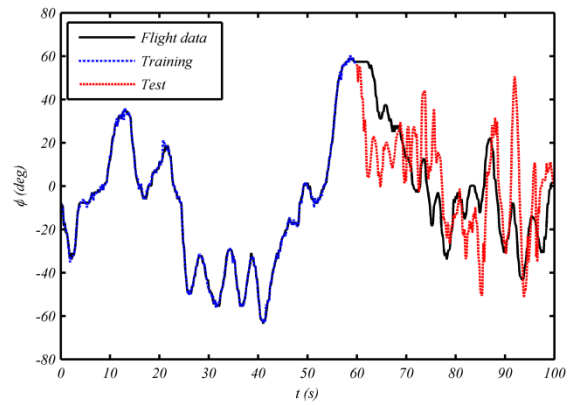
(d)

(e)

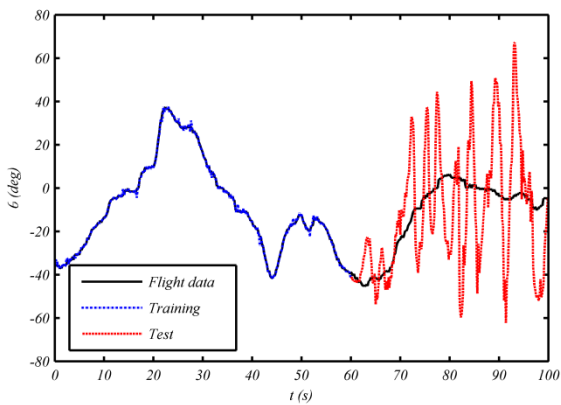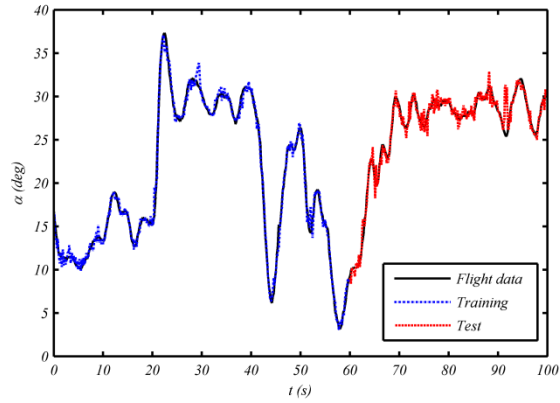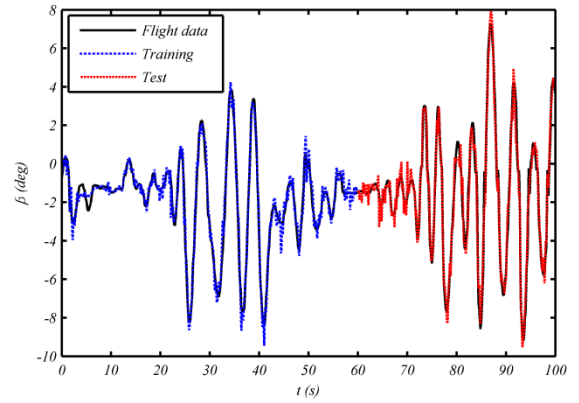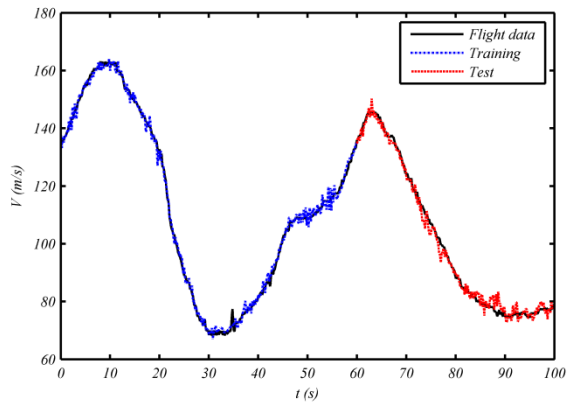**Fig. 11. The time-histories of the flight parameters acquired by the ANN**
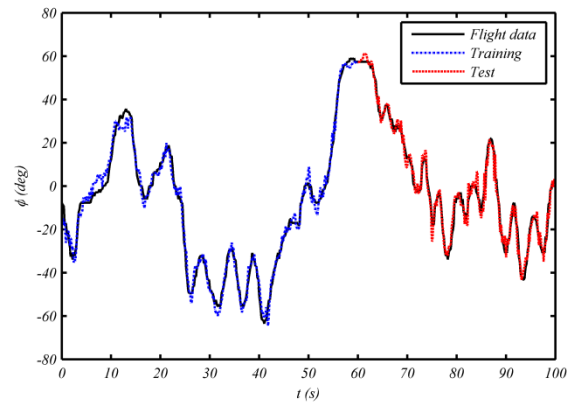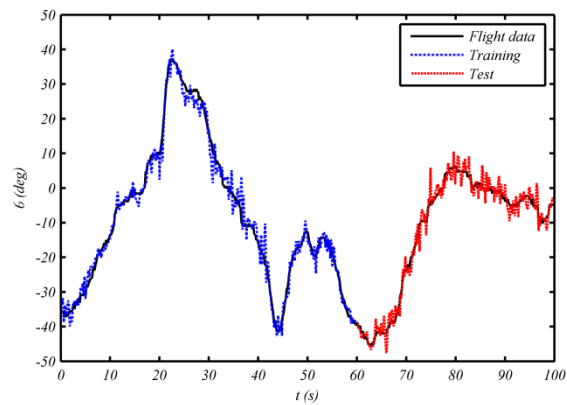
(a)

(b)

(c)

(d)

(e)

Fig. 12. The time-histories of the flight parameters acquired by the ANFIS

Table 4. The RMSE and FP for time-histories of the flight parameters estimated by the ANN model

	Training		Test	
	RMSE	FP	RMSE	FP
α	0.3262	96.1747	4.2155	18.6403
β	0.1401	93.8528	3.6298	-11.3126
V	0.5583	98.1968	18.6098	27.4844
ϕ	1.1627	96.1804	22.6248	13.5187
θ	0.7656	96.3799	26.0853	-55.7610

**Table 5. The RMSE and FP for time-histories of the flight parameters estimated by the ANFIS model**

	Training		Test	
	RMSE	FP	RMSE	FP
α	0.6283	92.6330	0.8388	83.8103
β	0.3869	83.0173	0.5569	82.9212
V	1.4898	95.1882	1.9501	92.4010
ϕ	3.3175	89.1022	3.1055	88.1296
θ	2.3658	88.8135	2.2313	86.6766

Table 6. The RMSE and FP for time-histories of the flight parameters estimated by the ANN and ANFIS for the flight test data acquired at the initial altitude of 17000 m
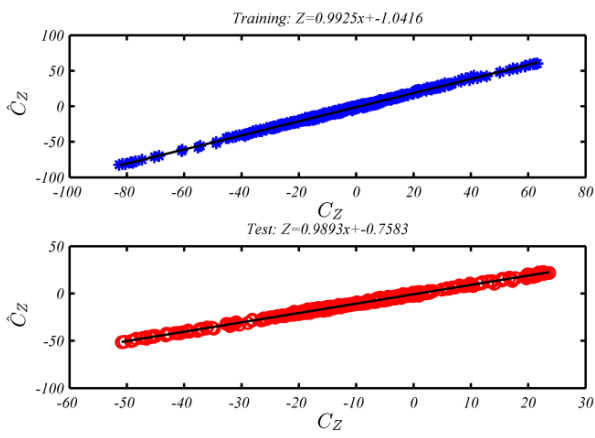
	ANN		ANFIS	
	RMSE	FP	RMSE	FP
α	15.9486	-178.7094	1.0321	81.9644
β	7.0204	-42.2666	0.9644	80.4570
V	46.5688	-189.9188	1.0425	93.5095
ϕ	40.8477	-25.6370	1.1019	96.6109
θ	44.2516	-62.5116	2.0735	92.3853
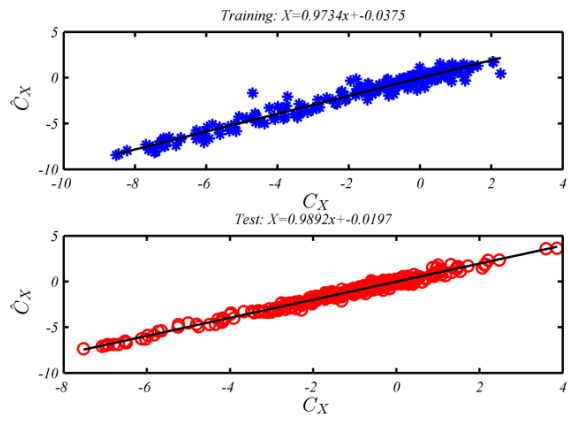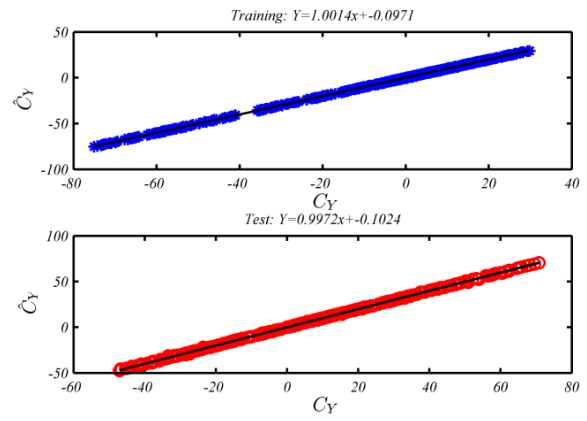
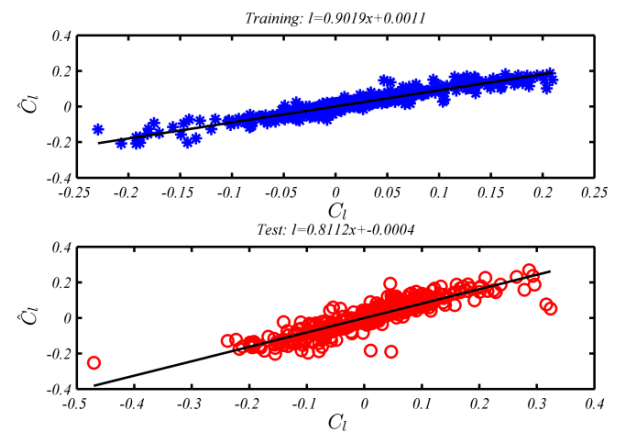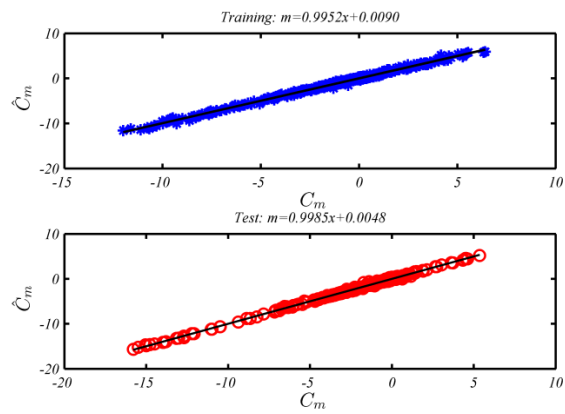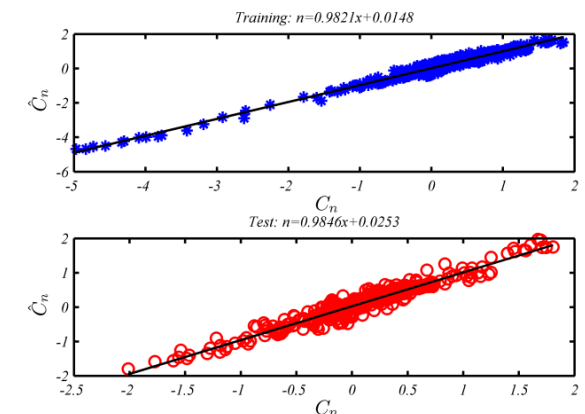**Fig. 13. The time-histories of the flight parameters acquired by the ANN and ANFIS for the flight test data acquired at the initial altitude of 17000 m**

The results indicate that ANN predictions cannot follow the non-trained flight data, and its results are thoroughly insignificant. Thus, one may conclude that ANN is not a suitable mathematical tool for the gray-box aircraft system identification from the generalization point of view. On the contrary, ANFIS model seems quite robust, and its performance is preserved in dealing with flight conditions dissimilar from the training ones. Hence, the ANFIS model has acceptable characteristics from both the precision and generalization viewpoints, and may be a reliable mathematical tool for the gray-box aircraft system identification.

5- Conclusion

The generalization is one of the most important characteristics of the models used for the aircraft system identification. To maintain the model fidelity, it should provide acceptable results for both the trained and non-trained inputs. While ANN is extensively used in the literature, it faces the over-fitting problem in dealing with the non-trained inputs. To overcome this weakness, the ANFIS structure is proposed to be implemented within a gray-box aircraft system identification process. The gray-box modeling employs equations of motion to estimate the force and moments instead of the flight parameters. Therefore, it may provide better generalization and precision. In this paper, flight test data of a large-scale unpowered RPV was analyzed by ANN and ANFIS models. Firstly, the precision of the training phase is examined. The results show that both of the models have ideal training properties. Afterwards, the models are examined for non-trained control commands at the flight conditions in which the training process is performed. The results indicate that ANN has moderate precision in the test phase, while ANFIS has excellent precision. Finally, the generalization of the model is studied in which both the flight conditions and control inputs are dissimilar from the training ones. The results indicate that the ANN predictions cannot follow the non-trained flight data while ANFIS seems quite robust. Since ANFIS model has acceptable characteristics from both the precision and generalization viewpoints, it may be a more reliable mathematical tool for the aircraft system identification. Further researches are needed to investigate the characteristics of the ANFIS model for this application.

References

[1] Batterson, J.G. and Klein, V., 1989. Partitioning of flight data for aerodynamic modeling of aircraft at high angles of attack. *Journal of Aircraft*, *26*(4), pp.334-339.

[2] Dias, J.N., 2015. Unsteady and Post-Stall Model Identification Using Dynamic Stall Maneuvers. In *AIAA Atmospheric Flight Mechanics Conference* (p. ۲۷۰۵).

[3] Klein, V., Batterson, J.G. and Murphy, P.C., 1981. Determination of airplane model structure from flight data by using modified stepwise regression. NASA Technical Publication (TP), NASA-TP-1916.

[4] Bagherzadeh, S.A., Sabzeparvar, M. and Karrari, M., 2015. Nonlinear aerodynamic model identification using empirical mode decomposition. *Proceedings of the Institution of Mechanical Engineers, Part G: Journal of Aerospace Engineering*, *229*(9), pp.1588-1605.

[5] Roudbari, A. and Saghafi, F., 2016. Generalization of ANN-based aircraft dynamics identification techniques into the entire flight envelope. *IEEE Transactions on Aerospace and Electronic Systems*, *52*(4), pp.1866-1880.

[6] Verma, H.O. and Peyada, N.K., 2020. Aircraft parameter estimation using ELM network. *Aircraft Engineering and Aerospace Technology*. 92(6), pp. 895-907.

[7] Sanwale, J. and Singh, D.J., 2018. Aerodynamic parameters estimation using radial basis function neural partial differentiation method. *Defence Science Journal*, *68*(3), p.241.

[8] Talwar, A., Lokhande, G., Jain, R. and Singh, S., 2017, August. Estimation of aerodynamic parameters using Cascade Forward Back Propagation. In *2017 2nd International Conference on Telecommunication and Networks (TEL-NET)* (pp. ۶-۱). IEEE.

[9] Mohamed, M. and Dongare, V., 2018. Aircraft neural modeling and parameter estimation using neural partial differentiation. *Aircraft Engineering and Aerospace Technology*. 90(5), pp. 764-778.

[10] Fan, H.Y., Dulikravich, G.S. and Han, Z.X., 2005. Aerodynamic data modeling using support vector machines. *Inverse Problems in Science and Engineering*, *13*(3), pp.261-278.

[11] Majeed, M. and Kar, I.N., 2013. Aerodynamic parameter estimation using adaptive unscented Kalman filter. *Aircraft Engineering and Aerospace Technology*. 85(4), pp. 267-279.

[12] Chowdhary, G. and Jategaonkar, R., 2010. Aerodynamic parameter estimation from flight data applying extended and unscented Kalman filter. *Aerospace science and technology*, *14*(2), pp.106-117.

[13] Göttlicher, C., Gnoth, M., Bittner, M. and Holzapfel, F., 2016. Aircraft parameter estimation using optimal control methods. In *AIAA Atmospheric Flight Mechanics Conference* (p. ۱۵۳۴).

[14] Saghafi, F. and Roudbari, A., 2014. Modeling and Identification of Fighter Aircraft Nonlinear Flight Dynamics, by Using Fuzzy Logic Algorithm. In *Proc. of the Scientific Cooperation's Intern. Workshops on Engineering Branches, Istanbul, Turkey* (pp. ۱۷-۹).

[15] Kouba, G., Botez, R.M. and Boely, N., 2010. Fuzzy logic method use in F/A-18 aircraft model identification. *Journal of aircraft*, *47*(1), pp.10-17.

[16] Hemakumara, P. and Sukkarieh, S., 2011, May. Non-parametric UAV system identification with dependent Gaussian processes. In *2011 IEEE International Conference on Robotics and Automation* (pp. ۴۴۳۵- ۴۴۴۱). IEEE.

[17] Mohammadi, S.J., Sabzeparvar, M. and Karrari, M., 2010. Aircraft stability and control model using wavelet transforms. *Proceedings of the Institution of Mechanical Engineers, Part G: Journal of Aerospace Engineering*, *224*(10), pp.1107-1118.

[18] Bagherzadeh, S.A., 2018. Nonlinear aircraft system identification using artificial neural networks enhanced

by empirical mode decomposition. *Aerospace Science and Technology*, *75*, pp.155-171.

[19] Verma, H.O. and Peyada, N.K., 2017, January. Modelling of aircraft's dynamics using least square support vector machine regression. In *International Conference on Mathematics and Computing* (pp. ۱۳۲- ۱٤۰). Springer, Singapore.

[20] Mengall G. Fuzzy modelling for aircraft dynamics identification. The Aeronautical Journal. 2001 Sep;105(1051):551-5.

[21] Roudbari, A. and Saghafi, F., 2017. Modeling and identification of highly maneuverable fighter aircraft dynamics using block-oriented nonlinear models. *Proceedings of the Institution of Mechanical Engineers, Part G: Journal of Aerospace Engineering*, *231*(7), pp.1293-1311.

[22] Lan, C.E., Li, J., Yau, W. and Brandon, J., 2002. Longitudinal and lateral-directional coupling effects on nonlinear unsteady aerodynamic modeling from flight data. In *AIAA Atmospheric Flight Mechanics Conference and Exhibit* (p. ٤۸۰٤).

[23] Kouba, G., Botez, R. M., & Boely, N., 2010. Fuzzy logic method use in F/A-18 aircraft model identification. Journal of aircraft, 47(1), pp.10-17.

[24] Jang, J.S., 1993. ANFIS: adaptive-network-based fuzzy inference system. *IEEE transactions on systems, man, and cybernetics*, *23*(3), pp.665-685.

[25] Roy, A.G. and Peyada, N.K., 2017(a). Aircraft parameter estimation using hybrid neuro fuzzy and artificial bee colony optimization (HNFABC) algorithm. *Aerospace Science and Technology*, *71*, pp.772-782.

[26] Roy, A.G. and Peyada, N.K., 2017(b). Lateral aircraft parameter estimation using neuro-fuzzy and genetic algorithm based method. In *2017 IEEE Aerospace Conference* (pp. ۱۱-۱). IEEE.

[27] Roy, A.G. and Peyada, N.K., 2017(c). Longitudinal aircraft parameter estimation using neuro-fuzzy and genetic algorithm based method. In *AIAA Atmospheric Flight Mechanics Conference* (p. ۳۸۹٦).

[28] Kumar, A. and Ghosh, A.K., 2019. ANFIS-Delta method for aerodynamic parameter estimation using flight data. *Proceedings of the Institution of Mechanical Engineers, Part G: Journal of Aerospace Engineering*, *233*(8), pp.3016-3032.

[29] Holleman EC., 1976. Summary of flight tests to determine the spin and controllability characteristics of a remotely piloted, large-scale (3/8) fighter airplane model. NASA Technical Note (TN). NASA-TN-D-8052.